



Cherenkov effects in radio emission from cosmic-ray induced air showers

KRIJN D. DE VRIES¹, AD M. VAN DEN BERG¹, OLAF SCHOLTEN¹, AND KLAUS WERNER²

¹*Kernfysisch Versneller Instituut, University of Groningen, 9747 AA, Groningen, The Netherlands*

²*SUBATECH, University of Nantes IN2P3/CNRS EMN, Nantes, France*

dvries@kvi.nl

DOI: 10.7529/ICRC2011/V02/0139

Abstract: We present a macroscopic calculation of Cherenkov effects in radio emission from cosmic-ray induced air showers. A high energy cosmic ray colliding in the atmosphere of the Earth produces a cascade of secondary charged particles. Due to different charge-separation mechanisms, coherent radio emission is emitted with a typical wave length of the size of this plasma cloud. The leading radio-emission mechanism is due to deflection of charged particles in the geomagnetic field. This deflection gives rise to a net current in the plasma cloud perpendicular to its motion. We describe a new type of Cherenkov radiation from a charge neutral current, which is due to the deviation of the index of refraction from unity in air. We show that the Cherenkov radiation strongly modifies the emission pattern at relatively short distances from the core of the shower, which offers a possibility for experimental verification.

Keywords: Extensive air showers; Radio emission; Magnetic Cherenkov radiation.

1 Introduction

Measurements of radio emission of cosmic ray-induced air showers at the LOPES [1], CODALMA [2], and more recently also at the Pierre Auger Observatory [3] have triggered the development of detailed models describing the radio-emission mechanism. We can separate two different types of models. On the one hand, there is the microscopic description, given by for example REAS3 [4]. These microscopic models add up the single-particle electric field contributions to obtain the full emission. On the other hand there is the macroscopic description originally proposed in [5], and in a renewed effort worked out in more detail by the MGMR (Macroscopic GeoMagnetic Radiation) model [6, 7, 8], and the EVA (Electric fields based on Variable index of refraction Air shower) model [9]. In the macroscopic approach, the relevant particle distributions and currents in the shower are used as input in Maxwell's equations to calculate the electromagnetic radiation. Recently it has been shown that both models are in good agreement [10, 11]. In this paper, we follow the macroscopic approach given by the MGMR and EVA models. When an ultra-high-energy cosmic ray enters the Earth's atmosphere, a cloud of secondary particles is created traveling toward the surface of the Earth with almost the speed of light. Charged particles inside this cloud are deflected by the Earth's magnetic field inducing a net transverse current. Time variation of this current leads to coherent radio emission over wavelengths of the typical size of the cloud, typically less than 1 m. In addition the knock-out of electrons from ambient air molecules, leads to a net varying

charge excess in the shower front emitting Askaryan radiation. The geomagnetic and Askaryan types of radiation can be distinguished by the observed polarization [8]. In this paper we address the effect of the index of refraction in air. As is well known, when a signal-emitting object is moving faster than the group velocity of the signal, a strong amplification of the emitted signal can be seen at certain angles by an observer in the medium. In the case of a single charge moving faster than the speed of light in the medium, defined by the vacuum speed of light divided by the index of refraction, c/n , this is the well-known Cherenkov radiation. In Ref. [9] it was already indicated that the deviation of the index of refraction from unity cannot be ignored in the modeling of radio emission from air showers, even though this deviation is extremely small. Such an effect is well-known in Cherenkov radiation, due to the Askaryan effect. Here we show that this effect also occurs for geomagnetic radiation.

2 Cherenkov effects in time domain

The index of refraction in air depends on the density, and therefore becomes a function of the height z from where the signal is emitted $n = n(z)$. A direct consequence of the height dependence of the index of refraction is that an emitted signal will not travel in a straight line. Therefore, we build our model by defining the distance along the light curve from the emission point to the observer, given by the integral $\int ds$, as $L(\vec{x}, \vec{\xi}(t'))$. At this point we can relate the negative shower time when the signal is emitted, $-t' =$

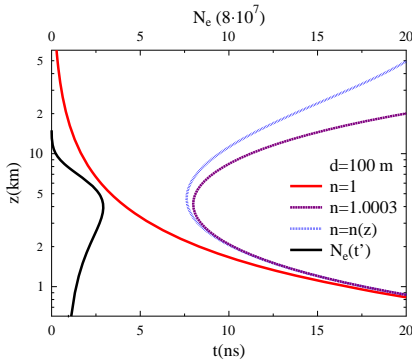


Figure 1: The emission height z as function of the observer time t for three different values of the index of refraction.

z/c defined by the height along the shower axis divided by the speed of light, to the observer time t by the light-cone constraint

$$c(t - t') = L(\vec{x}, \vec{\xi}(t')). \quad (1)$$

Here \vec{x} is the observer position with respect to the impact point of the shower front on the Earth's surface, and $\vec{\xi}(t') = (\vec{r}_\perp, -ct' + h)$ is the source position from where the signal is emitted. Here \vec{r}_\perp is the lateral distance from the shower front, and h is the longitudinal distance behind the shower front which moves, by definition, with the speed of light along the shower axis. By definition, $t = t' = 0$ when the shower hits the Earth's surface.

At this point we focus on the emission height $z = -ct'$, where the signal is emitted, as a function of the observer time t when the signal is received. We do this for a fixed geometry of a $5 \cdot 10^{17} eV$ air shower with a zenith angle of $\theta = 27$ degrees seen by an observer at a distance of 100 meters from the impact point of the shower. In Fig. 1, the emission height is plotted as a function of the observer time. First we discuss the case for an index of refraction equal to unity, $n = 1$. In this case a signal travels with the same speed as the shower front. Now imagine two signals. The first signal is emitted at a large height and from there moves along a straight line towards the observer. The second (fictive) signal is emitted at a smaller height (later time), so we can imagine that this signal first has to travel along with the shower before it is emitted and from there on will move along a straight line towards the observer. Hence the second signal has to travel a longer distance and arrives at a later time. So signals emitted from large heights arrive before signals emitted in a later stage of the shower for an index of refraction equal to unity. This can be seen by the full (red) line in Fig. 1. The situation is different for an index of refraction larger than unity. In this case, even though the signal that is emitted at a larger height has to travel a shorter distance, its average speed will be the speed of light in the medium, c/n . The second (fictive) signal moving along with the shower before it is emitted at a later time, first moves at the speed of the shower itself, c , before it is emitted and from there on moves with the

speed of light in the medium c/n . Therefore the average speed becomes larger for the second (fictive) signal than the average speed of the signal emitted at an earlier time. As a consequence, both signals could arrive at the same time at the observer. This is shown by the dashed (purple) line in Fig. 1, for $n = 1.0003$, and by the dotted (blue) line in Fig. 1 for a realistic index of refraction depending on height $n = n(z)$. For later use, we also plotted the shower profile as a function of the negative retarded shower time in Fig. 1.

From the discussion above, we conclude that in case of a realistic value for the index of refraction, there will be one unique position, acting as the first point from which the emission seems to originate. From Fig. 1, we see that this position corresponds to an ideal time which we will call t_c , where the time derivative $dz/dct = -dt'/dt$ diverges. The meaning of this divergence is that at this exact time we do not see an infinitesimal signal any more, but all signals emitted around the height corresponding to the Cherenkov time arrive at the same time at the observer and hence the signal becomes enhanced. We can calculate the Cherenkov times t_c and t'_c for a fixed constant index of refraction, which become

$$t_c = d\sqrt{n^2\beta^2 - 1} \quad (2)$$

$$t'_c = d/\sqrt{n^2\beta^2 - 1}. \quad (3)$$

The critical emission time corresponds to a critical emission height, $z_c = -ct'_c$, leading to the familiar expression for the Cherenkov angle, $\cos(\theta_c) = 1/(n\beta)$. Note that the above discussion was done for electromagnetic radiation, but can also be applied, for example, to sound waves (sonic boom) or a "bow wave" of a moving ship.

3 Cherenkov effects for geomagnetic radiation

We saw in the previous sections that the Cherenkov effect is due to geometry leading to the divergence of the derivative $dz/dct = -dt'/dt$, so it should equally well apply to geomagnetic radiation from a net charge-less current, our case, as to the radiation from a net charge moving faster than the speed of light in the medium, to the Askaryan effect. We start our model with the Liénard-Wiechert potentials from classical electrodynamics,

$$A_{PL}^\mu(t, \vec{x} - \vec{\xi}(t')) = \frac{\mu_0}{4\pi} \frac{J_{PL}^\mu}{|\mathcal{D}|} \Big|_{t=t'}, \quad (4)$$

that have to be evaluated at the shower time t' . The potentials are given for a point-like approximation, where the currents induced in the shower front are defined as

$$J_{PL}^\mu = J^\mu(t')\delta^3(\vec{x} - \vec{\xi}(t')). \quad (5)$$

The current is proportional to the total number of particles in the shower, $J^\mu(t') \propto N_e(t')$ for the case of geomagnetic radiation. In the previous section we showed that

Cherenkov effects occur at the point where the time derivative dt'/dt diverges. Mathematically, this is expressed by the retarded distance \mathcal{D} which can be linked to the time derivative of the retarded time by $\mathcal{D} = L/(dt'/dt)$ [9]. It follows that at the Cherenkov time, t_c , the retarded distance vanishes and the vector potential diverges. To solve for the vector potential, we have to include the finite extent of the shower. The vector potential now becomes

$$A_w^\mu(t, \vec{x} - \vec{\xi}(t')) = \int d^2\vec{r} \int dh \rho(\vec{r}, h) A_{PL}^\mu(t, \vec{x} - \vec{\xi}(t')), \quad (6)$$

where $\rho(\vec{r}, h)$ defines the lateral and longitudinal distribution of the particles in the shower front and can be expressed by

$$\rho(\vec{r}, h) = 2\pi r w(r, h) = 2\pi r w_1(r) w_2(r, h). \quad (7)$$

Here $w_1(r)$ defines the lateral distribution of the particles, and $w_2(r, h)$ defines the longitudinal distribution of the particles as a function of the radial distance r .

The electromagnetic fields are now obtained through the standard relation

$$E^i(\vec{x}, t) = -\frac{d}{d\vec{x}} A^0(\vec{x}, t) - \frac{d}{dct} A^i(\vec{x}, t) \quad (8)$$

By a shift in coordinates such that the derivatives only work on the particle distributions, we now obtain the electric field which for pure geomagnetic radiation is given by

$$E^i(\vec{x}, t) = -\frac{\mu_0 c}{4\pi} \int d^2\vec{r} \int dh \frac{1}{|\mathcal{D}|} \times \left[\frac{\partial w(r, h)}{\partial h} J_{PL}^i(t') + w(r, h) \frac{\partial J_{PL}^i(t')}{\partial t'} \right]. \quad (9)$$

We see that Eq. (9) consists of two terms over which is integrated. The first term inside the brackets is a convolution of the total current, $\vec{J} \propto N_e(z)$, and the longitudinal derivative of the weight function, $\partial w(r, h)/\partial h$. The second term scales with the derivative with respect to the retarded time of the shower profile $\partial J_{PL}^i/\partial t' \propto \partial N_e(t')/\partial t'$, which is convoluted with the weight function $w(r, h)$. Both terms in Eq. (9) scale with $1/|\mathcal{D}| = (dt'/dt)/L$. If we now look at the two terms in Eq. (9), we see that for a slowly varying value of $1/|\mathcal{D}|$ the first term is an integral over the longitudinal derivative of our weight function and thus becomes small while the second term in Eq. (9) becomes leading. This is the case for an index of refraction equal to unity, as can be seen from Fig. 1. Nevertheless, when we look at Fig. 1, we see that the retarded distance changes very rapidly around the critical Cherenkov time. Therefore, at these critical times the first term in Eq. (9) becomes the leading term, and a strong enhancement of the emitted signal is seen. So it is this first term, which scales to the total number of particles in the shower $N_e(z)$, which is responsible for the Cherenkov effect. Here it should be noticed that we see Cherenkov radiation from a charge-neutral geomagnetic current. We will refer to this specific type of radiation as magnetic Cherenkov radiation.

4 Results

We saw from the previous sections that there are two effects that we should observe when simulating the electric field induced by an extensive air shower. The first effect is that the pulse will arrive at a later time for an index of refraction larger than unity. The second effect is that we expect to see a strong amplification of our electric field strength at the critical Cherenkov time due to a vanishing retarded distance. To study the effects of an index of refraction larger than unity, we will consider the full current to be distributed in a single line and neglect the lateral spread of the particles in the shower front, hence $w(\vec{r}, h) = \delta(\vec{r})w(h) = \delta(\vec{r})(4/L^2)he^{-2h/L}$, where $w(h)$ is chosen to fit measured arrival time distributions [13], and $L = \langle h \rangle = 0.5$ is chosen to give more weight to the shower core following CONEX-MC-GEO simulations [9]. In Fig. 2, the electric field is plotted for a $5 \cdot 10^{17}$ eV air shower coming in at a zenith angle of 27 degrees as seen by an observer at a distance of 100 meters from impact point of the shower. As we would expect from Fig. 2 it follows that the pulse for a realistic index of refraction, $n = n(z)$, arrives slightly before the pulse seen for a constant index of refraction at sea level $n = 1.0003$, but a relatively long time after the pulse observed for an index of refraction equal to unity, $n = 1$. Because the second term in Eq. (9) leads for an index of refraction equal to unity we expect to see the maximum electric field strength at the time where the maximum of the derivative of the shower profile is seen. This maximum occurs at around 3 ns, which is in agreement with the position of the maximum field strength for $n = 1$ in Fig. 2.

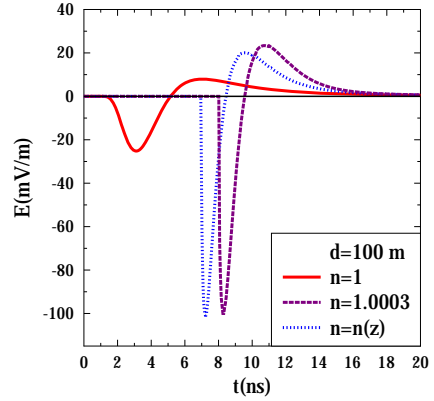


Figure 2: The electric field due to geomagnetic radiation for a $5 \cdot 10^{17}$ eV inclined air shower with a zenith angle of 27 degrees as seen by an observer at a distance of 100 m from the core for different values of the index of refraction, $n = 1$, $n = 1.0003$ fixed, and $n = n(z)$. Ignoring the lateral extent of the shower front.

4.1 Experimental verification and chemical composition

Fig. 3 shows the electric field including the lateral extent of the shower front, $w(r)$, which is fitted by CONEX-MC-GEO simulations [9]. In this figure the electric field is given at several distances from the shower core. There is a strong enhancement of the electric field at around 100 meters from the shower axis. This enhancement is seen because the critical height corresponding to Cherenkov emission is equal to the height of the shower maximum. For an observer positioned closer to the shower axis, the critical height corresponding to Cherenkov emission is equal to the height where the shower is already beyond the shower maximum, and the effect diminishes. This enhancement is also shown in Fig. 4, where the Lateral Distribution Function (LDF) is plotted of the maximum pulse strength for the three choices of the index of refraction. In this plot we scaled the maximum field strength with the square-root of the distance to keep the LDF for $n = 1$ on a reasonable scale. Fig. 4 shows that the LDF for an index of refraction deviating from unity peaks at distances where Cherenkov effects are large close to the shower maximum, and we obtain a direct handle on the position of the shower maximum, which itself is a measure for the composition of the primary particle. Fig. 4 shows a clear difference between the $n = 1$ case, where the LDF peaks to $d = 0$, and the case of an index of refraction deviating from unity where the LDF peaks at a finite distance. First hints of Cherenkov effects might have been seen already by the LOPES collaboration [14], but a more detailed analysis is needed taking into account interference effects due to the different polarization behavior of the geomagnetic and Askaryan type of radiation.

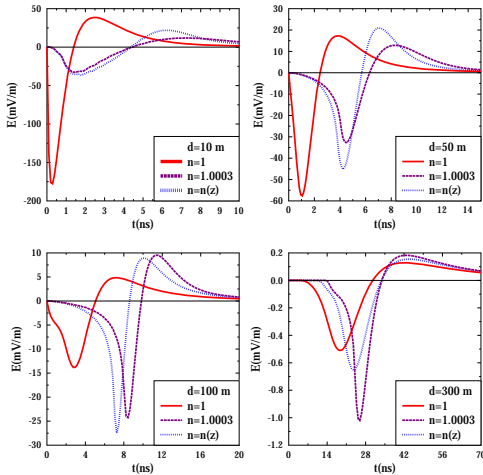


Figure 3: The electric field due to geomagnetic radiation at several distances from the shower axis for different values of the index of refraction, $n = 1$, $n = 1.0003$, and $n = n(z)$, including the lateral extent of the shower.

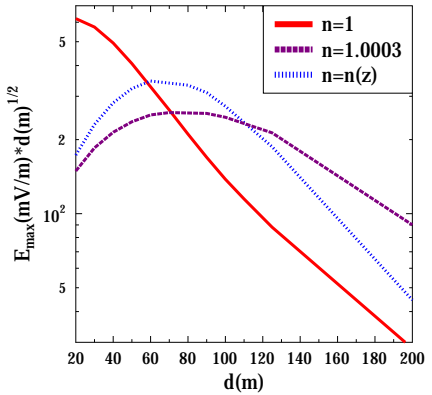


Figure 4: Pulse LDF for the three choices for the index of refraction, $n = 1$, $n = 1.0003$, and $n = n(z)$.

References

- [1] W.D. Apel *et al.*, Astropart. Phys., 2006, **26**:332
- [2] D. Arduin and the CODALEMA Collaboration, Astropart. Phys., 2009, **31**:192
- [3] B. Revenu [Pierre Auger Collaboration], this conference; J.L. Kelley [Pierre Auger Collaboration], this conference.
- [4] M. Ludwig and T. Huege, proceedings of ARENA 2010; Nucl. Instr. and Meth. A (in print), 2010, doi:10.1016/j.nima.2010.10.115
- [5] F.D. Kahn and I. Lerche, Proc. Royal Soc. London, 1966, **A289**:206
- [6] Olaf Scholten, Klaus Werner, and Febdian Rusydi, Astropart. Phys., 2008, **29**:94
- [7] Olaf Scholten and Klaus Werner, Nucl. Instr. and Meth. A, 2009, **604**:24-26
- [8] K.D. de Vries *et al.*, Astropart. Phys., 2010, **34**:267
- [9] K. Werner and O. Scholten, Astropart. Phys., 2008, **29**:393
- [10] T. Huege *et al.*, proceedings of ARENA 2010; Nucl. Instr. and Meth. A (in print), 2010, doi:10.1016/j.nima.2010.11.041.
- [11] M. Ludwig, T. Huege, O. Scholten, and K.D. de Vries, A detailed comparison of MGMR and REAS3, this conference.
- [12] J.D. Jackson: 1999, Classical Electrodynamics, Wiley, New York
- [13] G. Agnetta *et al.*, Astropart. Phys., 2003, **6**:301
- [14] W.D. Apel *et al.*, Astropart. Phys., 2010, **32**:294